

# IMPACT OF A MAGNETIC FIELD ON GRAIN BOUNDARY ENERGY IN 99.9% IRON AND IRON-TIN ALLOY

R. Sumi<sup>1</sup>, N. Toda<sup>1</sup>, H. Fujii<sup>1\*</sup> and S. Tsurekawa<sup>1</sup>

<sup>1</sup>Department of Materials Science and Engineering, Graduate School of Science and Technology, Kumamoto University, 860-8555, Kumamoto, Japan

\*On leave from Department of Nanomechanics, Graduate School of Engineering, Tohoku University, 980-8579, Sendai, Japan

Received: December 20, 2008

**Abstract.** We have investigated the effect of a magnetic field on grain boundary energy in a 99.9% Fe and an Fe-0.8at.%Sn alloy. The average grain boundary energy in the Fe-Sn alloy was increased by application of a magnetic field. The energy curves as a function of misorientation angle showed cusps at the angles corresponding to CSL relations irrespective of whether a magnetic field was applied. The misorientation dependence of grain boundary energy was more observable after magnetic annealing, probably because of a decrease in Sn segregation to grain boundaries due to a magnetic field. Temperature-dependence of grain boundary energy in 99.9% Fe was measured. The grain boundary energy increased linearly with increasing temperature without a magnetic field, while it decreased with a 6 T magnetic field. The difference in temperature coefficient of grain boundary energy observed would come from the magnetic-field effect on the impurity segregation. Furthermore a discontinuity of temperature dependence of grain boundary energy was found at the Curie temperature under a 6 T magnetic field.

## 1. INTRODUCTION

Grain boundary energy often exerts influences on not only microstructural evolution but also mechanical properties of polycrystalline materials. The energy can act as a driving force for grain boundary migration, particularly in secondary recrystallization [1], and governs intergranular fracture in intrinsically brittle materials like molybdenum [2], for example. Many experimental and theoretical studies have evidenced that grain boundary energy considerably depends not only on the misorientation between two adjoining grains but also the inclination of grain boundary plane [3-8]. In addition, grain boundary energy has been found to vary significantly with solute / impurity segregation to grain boundaries [9,10]. Hondros derived theoretically the

relation between grain boundary energy and the amount of solute / impurity segregation by applying the Gibbs adsorption theorem, and showed that grain boundary energy decreases with increasing grain boundary segregation [11].

Recently a new strategy for controlling microstructure by application of a magnetic field has been proposed. A magnetic field has been found to affect many metallurgical phenomena, such as recrystallization [12-17], grain growth [18-20], phase transformation [21-25]. Tsurekawa *et al.* have found that a magnetic field can suppress tin segregation to grain boundaries in Fe-Sn alloys, and the resultant grain boundary energy increased [26]. Although grain boundary energy can depend on grain boundary character / structure, the influence of a mag-

Corresponding author: S. Tsurekawa, e-mail: [turekawa@kumamoto-u.ac.jp](mailto:turekawa@kumamoto-u.ac.jp)

netic field on the misorientation dependence of grain boundary energy was not clarified. In addition, it is still unclear about the increase in grain boundary energy in the Fe-Sn alloy by magnetic annealing, that is, whether it is an extrinsic effect resulting from a decrease in tin segregation to grain boundaries, or whether it is an intrinsic effect of a magnetic field on grain boundary energy. Furthermore, it is interesting to study the influence of magnetic transformation on grain boundary energy. These motivated us to further study the magnetic field effect on grain boundary energy in pure Fe and Fe-Sn alloy.

## 2. EXPERIMENTAL

### 2.1. Sample preparation

An Fe-0.8at.%Sn alloy was prepared by vacuum melting an electrolytic iron with a high purity tin (99.999% in purity). The ingot was hot-forged and then hot-rolled into a sheet with 1 mm in thickness at 873K. Specimens for magnetic annealing with dimensions of 10mm × 6mm × 1mm were cut from the sheet using a spark cutter, and mechanically polished using waterproof SiC papers, buff-finished to the mirror surface by colloidal silica.

A 99.9% Fe was cold-rolled to plate with a reduction rate of 86.5%. Specimens with 13mm × 7mm × 0.7mm in dimensions were cut and polished with the same way as the Fe-Sn samples. Thereafter, they were annealed at 1163K for 24 h in a vacuum of 1 mPa for recrystallization and grain growth, and then subjected to SEM/EBSD observations for determination of grain boundary character.

### 2.2. Magnetic annealing and microstructural evaluation

The relative grain boundary energies were determined by equilibrium configuration of grain boundary grooves. In order to develop grain boundary grooves, the Fe-0.8 at.%Sn and the 99.9% Fe were annealed at 973K, and at temperatures ranging ferromagnetic and paramagnetic states, respectively, for 6h in a vacuum of  $6 \cdot 10^{-4}$  Pa without and with a magnetic field up to 6 T using a specially designed superconducting magnetic field heating system ( $H_{\max} = 6$  T,  $T_{\max} = 1873$ K). The direction of the magnetic field was parallel to the rolling direction.

Grain boundary microstructure was examined using an automated SEM/EBSD system. The EBSD observations were conducted on a Hitachi

cold FEG-SEM (S4200) equipped with TSL's OIM system at an accelerating voltage of 20 kV. The electron beam was scanned on the surface using a 6–15  $\mu\text{m}$  step size.

### 2.3. Measurements of grain boundary energy

Atomic force microscope (AFM), SHIMADZU SPM-9500, was used to measure the cross-sectional profiles of grain boundary grooves formed during ordinary and magnetic annealing in order to evaluate grain boundary energy. Grain boundary energy was evaluated by,

$$\gamma_{gb} = 2\gamma_s \cos(\theta / 2), \quad (1)$$

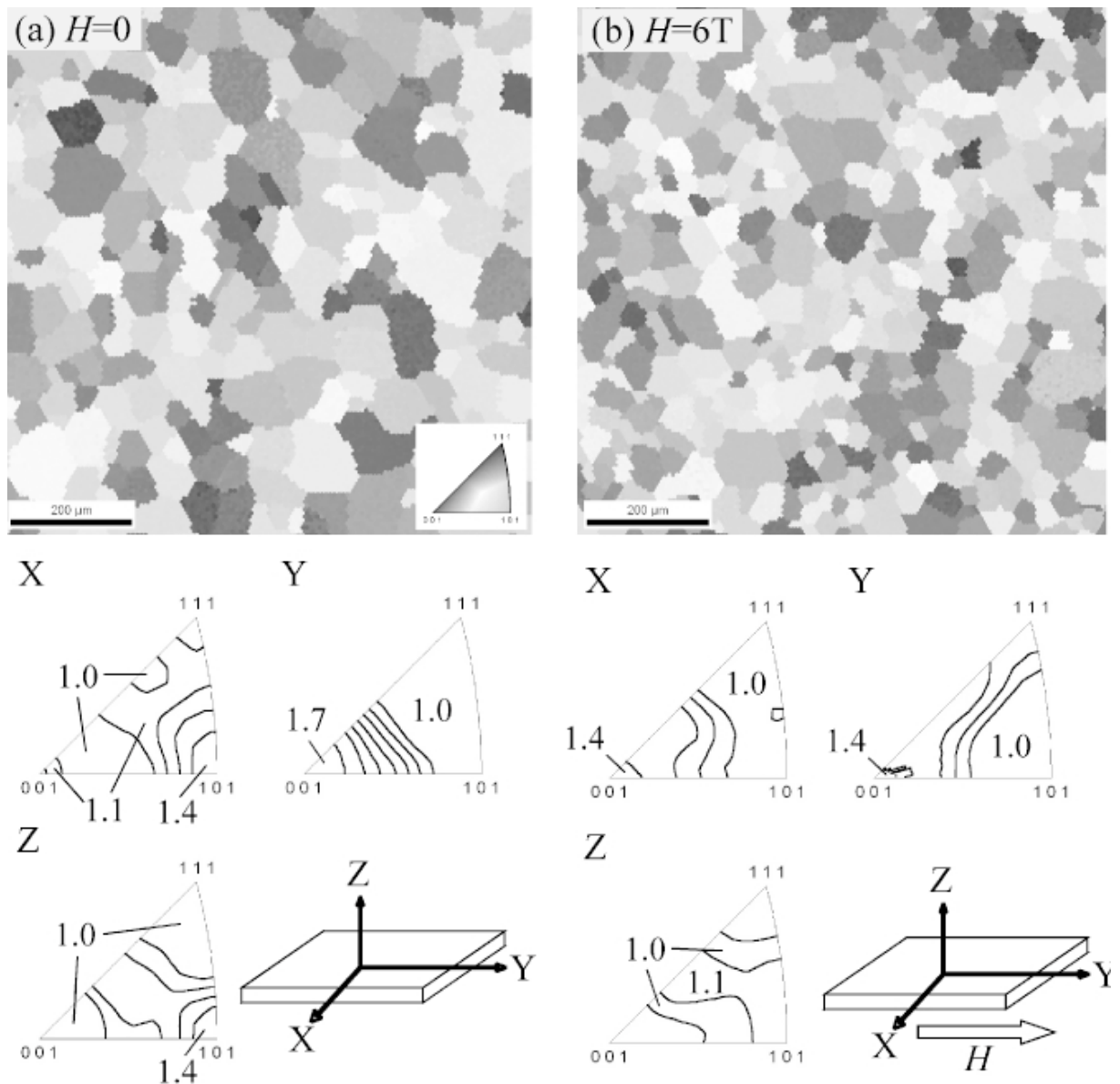
where  $\gamma_{gb}$  and  $\gamma_s$  are the grain boundary energy and the surface energy, respectively, and  $\theta$  is a dihedral angle of a grain boundary groove. The AFM measurements were carried out on well-characterized grain boundaries. The dihedral angles were measured at four different positions along a grain boundary and such measurements were performed for 16 different boundaries in Fe-Sn alloy. In case of the 99.9% iron, they were measured at 12~40 different positions along a grain boundary for 19~50 different boundaries.

## 3. RESULTS AND DISCUSSION

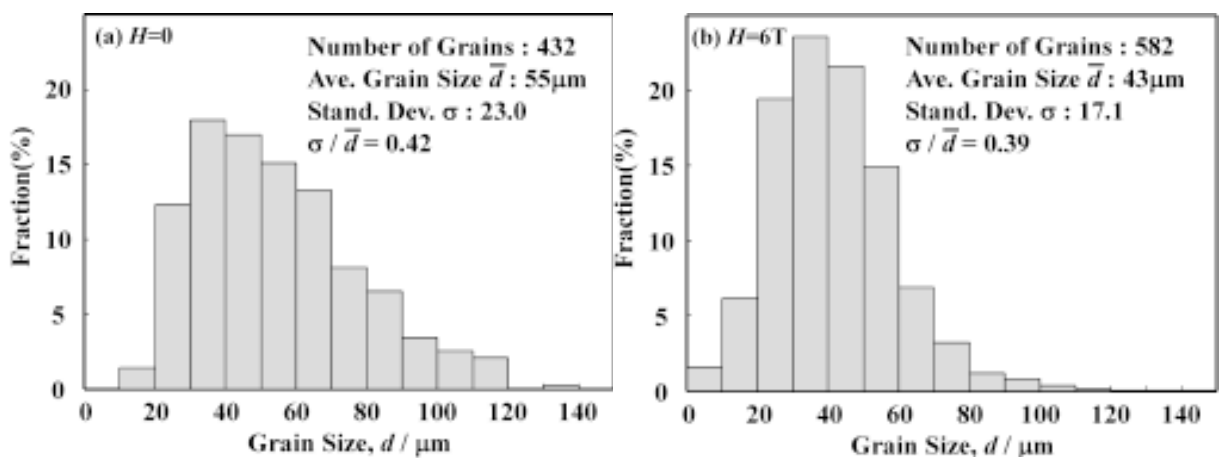
### 3.1. Effect of a magnetic field on grain boundary microstructure in Fe-Sn alloy

Fig. 1 presents OIM micrographs showing the grain orientations perpendicular to the surface and the inverse pole figures for the Fe-Sn alloy annealed (recrystallized) at 973K for 6 h (a) without and (b) with a 6 T magnetic field. There is no significant sign for texture formation irrespective of whether magnetic field was applied. However, it is evident that the grain size is decreased by application of a magnetic field. The grain size distributions of them are shown in Fig. 2, which reveals that a magnetic field can give rise to not only a decrease in the average grain size but also development of homogeneous microstructure, as recognized by decreasing the standard deviation of grain size distribution. Martikainen and Lindroos found that recrystallization was retarded in a magnetic field [13]. This is a possible reason for the decrease in grain size for the Fe-Sn alloy recrystallized in a magnetic field.

Fig. 3 shows the grain boundary character distributions in an Fe-0.8at.%Sn alloy annealed at



**Fig. 1.** OIM micrographs showing grain orientation perpendicular to the surface and the inverse pole figures for an Fe-0.8at.%Sn alloy annealed at 973K for 6h (a) without and (b) with a 6 T magnetic field.



**Fig. 2.** Grain size distributions for a Fe-0.8at.%Sn alloy annealed at 973K for 6h (a) without and (b) with a 6 T magnetic field.

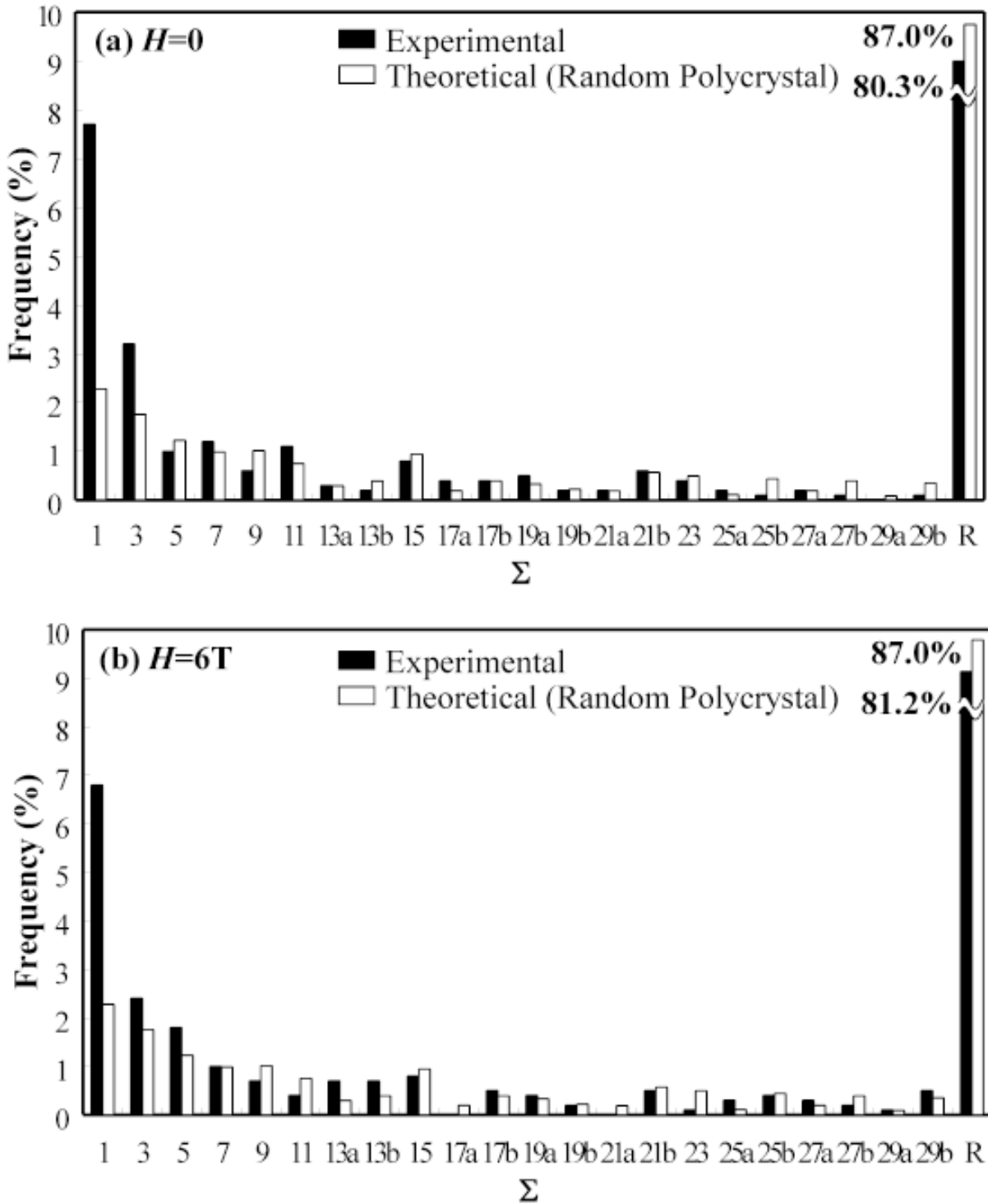


**Fig. 3.** Grain boundary character distributions in an Fe-0.8at.%Sn alloy annealed at 973K for 6h (a) without and (b) with a 6T magnetic field.

973K for 6 h (a) without and (b) with a 6 T magnetic field. It is found that the fraction of low angle boundaries is higher than the theoretical value for a random polycrystal irrespective of whether a

magnetic field is applied. Watanabe *et al.* have found that the fraction of CSL boundaries increases with increasing a magnetic field for an Fe-9at.%Co alloy [14]. However we could not find an observ-

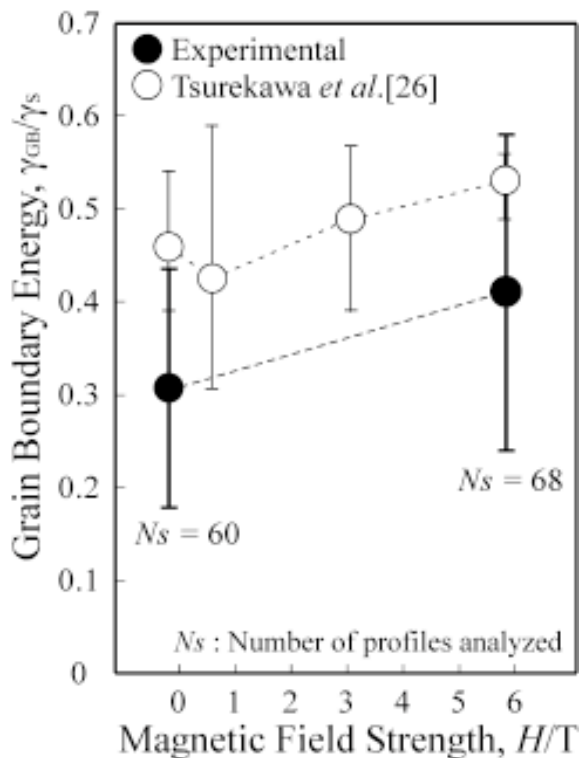


**Fig. 4.** Grain boundary energy in an Fe-0.8at.%Sn alloy as a function of a magnetic field applied during annealing at 973K.

able change in grain boundary character distributions in the Fe-0.8at.%Sn alloy with application of a magnetic field.

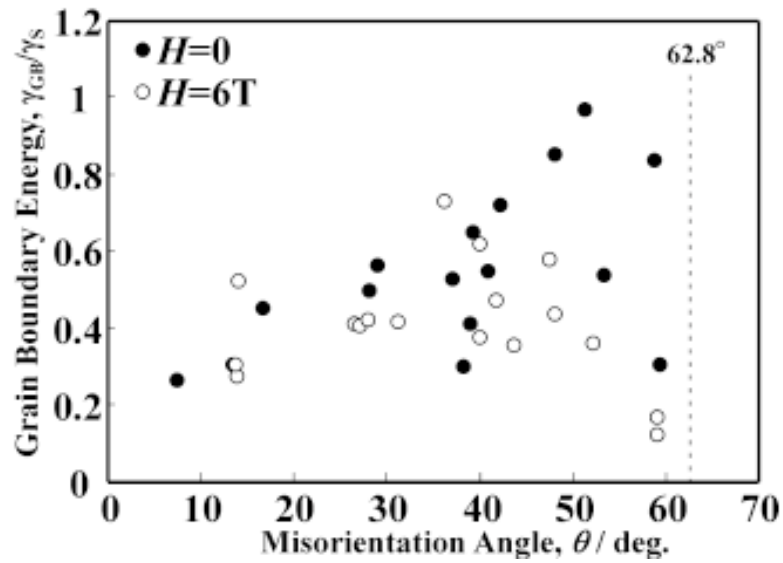
### 3.2. Effect of magnetic field on grain boundary energy in Fe-Sn alloy

Fig. 4 shows the average grain boundary energy in the Fe-0.8at.%Sn alloy as a function of a magnetic field applied during annealing. Here, Ns stands for the total number of cross-sections analyzed. For comparison, the data from the previous study [26] were shown in Fig. 4. The average grain boundary energy is found to increase in a magnetic field, as is consistent with the previous report, though the absolute values of grain boundary energies are lower [26]. A large variety of the data would come from the difference in grain boundary energy depending on grain boundary character. Accordingly, it is important to understand how the misorientation-dependent grain boundary energy is affected by a magnetic field. Fig. 5 shows the grain boundary energy in the Fe-0.8at.%Sn samples annealed 973K without and with a 6 T magnetic field as a

function of misorientation angle obtained from the OIM. The energies tend to increase with increasing misorientation, and show a maximum around 50 degree and 40 degree without and with a 6 T magnetic field, respectively. However, there seems to be no significant relationship between grain boundary energy and misorientation angle even for the case without a magnetic field. This is probably because the rotation axis for each grain boundary was not distinguished in Fig. 5. The OIM software only dictates the minimum angle as a misorientation from the 24 equivalent variants of angle / rotation axis pairs. Accordingly, we assessed the 24 angle/axis pairs of each grain boundary, and examined the boundaries with respect to a  $\langle 110 \rangle$  or  $\langle 111 \rangle$  rotation axis. Here, the tolerance angle of rotation axis from the exact direction interested was defined as 5 degree. Figs. 6a and 6b show the grain boundary energy as a function of misorientation angle around the  $\langle 110 \rangle$  and  $\langle 111 \rangle$  rotation axis, respectively, in the Fe-0.8at.%Sn samples annealed at 973K without and with a 6 T magnetic field. It is found that the misorientation vs grain boundary energy curves tend to possess cusps at the angles corresponding to CSL relations, irrespective of whether a magnetic field was applied. Of particular importance is the finding that an increase in grain boundary energy due to the magnetic field is different according to grain boundary character: the increase in the energy is much smaller at the low-energy  $\Sigma 3$  boundary than at the other boundaries. As the result, misorientation dependence of grain boundary energy in a magnetic field became more significant. Sautter *et al.* [10] have suggested that impurity segregation reduces the energy of high energy boundaries more than the energy of low energy boundaries, and then energy of low and high energy boundaries is equalized with increasing impurity segregation. Because Sn segregation to grain boundaries in the Fe-Sn alloy will be suppressed by a magnetic field, as experimentally confirmed [26], the results shown in Fig. 6 agree with the suggestion of Sautter *et al.*[10].

### 3.3. Temperature dependence of grain boundary energy in 99.9% Fe under a magnetic field

Fig. 7 shows the grain boundary energy in 99.9% Fe under (a) non-field and (b) a 6 T magnetic field as a function of temperature. The values of Ns represent the total number of cross-sections of grain boundary grooves analyzed. Fig. 7a reveals that grain boundary energy in the 99.9% Fe increases



**Fig. 5.** Grain boundary energy vs the minimum rotation angle as misorientation for an Fe-0.8%Sn alloy without and with a 6 T magnetic field.

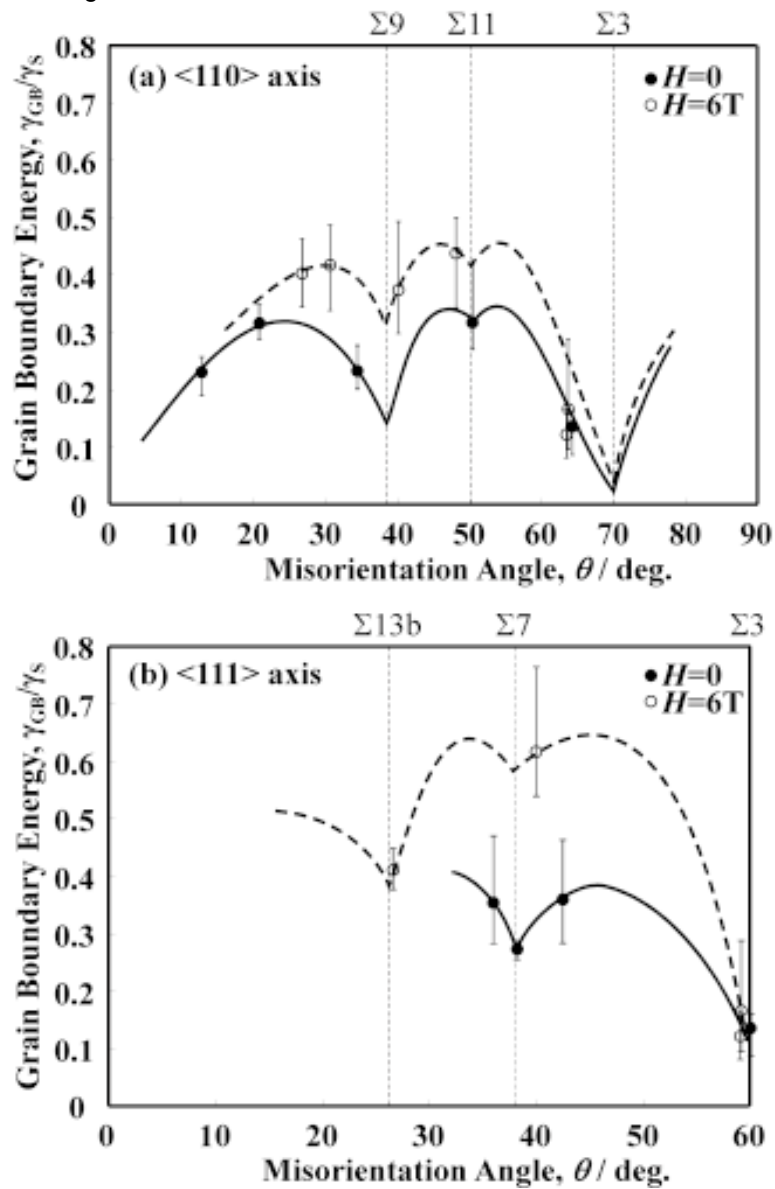


**Fig. 6.** Grain boundary energy vs misorientation angle for an Fe-0.8%Sn alloy without and with a 6 T magnetic field (a)  $\langle 110 \rangle$  and (b)  $\langle 111 \rangle$  rotation axis.

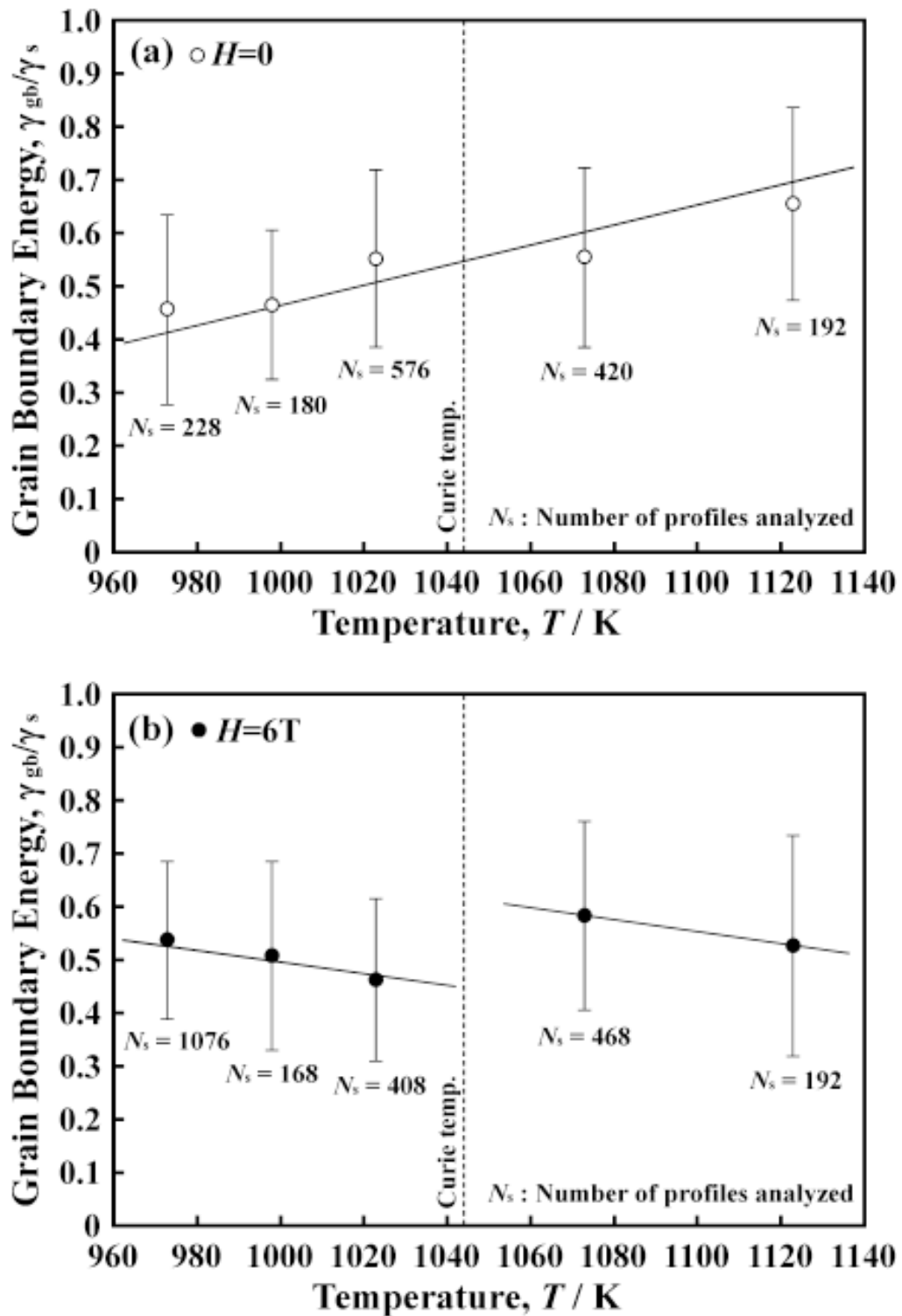


**Fig. 7.** Temperature dependence of grain boundary energy in 99.9% Fe (a) without and (b) with a 6 T magnetic field.

with increasing temperature under a non-field. Generally speaking, grain boundary energy in pure metals shows a “negative” temperature-dependence according to  $(d\gamma/dT)_v = -S_p$  where  $S_p$  is the

interfacial entropy [6]. On the other hand, grain boundary energy in metals with alloying elements and/or impurities often shows the “positive” temperature dependence due to solute / impurity seg-

regation to grain boundaries [27]. This is because the negative entropy of segregation, as observed in Fe-Si alloy [28] for example, would compensate the positive entropy in pure grain boundaries. Therefore, the positive temperature-dependence of grain boundary energy observed in 99.9% Fe may have been attributed to impurity segregation. From ICP qualitative analyses, the 99.9% iron used in this study was found to include Si, Mn, Co, Cu as impurities. Conversely, the temperature dependence of grain boundary energy became "negative" under a 6 T magnetic field as shown in Fig. 7b. As mentioned in the previous section, a magnetic field can suppress impurity segregation to grain boundaries. Accordingly, Fig. 7b is likely to reveal intrinsic nature of temperature-dependent grain boundary energy in Fe under a magnetic field without any influences of impurities.

From Fig. 7, we obtained the temperature coefficients for grain boundary energies to be 2.8 mJ/m<sup>2</sup>K (19.1 J/molK) and -4.4 mJ/m<sup>2</sup>K (-30.5 J/molK) under a non-magnetic field and a 6 T magnetic field, respectively. Assuming that the entropy compensation mentioned above is the case, the entropy of segregation can be estimated to be approximately 50 J/molK (we assumed the width of grain boundary to be 1 nm), This estimated value seems to be a reasonable for a entropy of grain boundary segregation [29].

In addition, it is worthy to note that the magnetic transformation can affect the grain boundary energy: the grain boundary energy discontinuously increased with increasing temperature around the Curie temperature under a 6 T magnetic field. The discontinuity of grain boundary energy observed might be explained by the difference between energetic contribution from the applied magnetic field to Gibbs free energy in the ferromagnetic state and that in the paramagnetic state.

#### 4. CONCLUSIONS

We have studied the influence of an applied magnetic field on the dependences of temperature and misorientation on grain boundary energy in a Fe-0.8 at.%Sn alloy and 99.9% Fe. The chief results obtained are as follows.

- (1) Recrystallization of the Fe-Sn alloy under a magnetic field decreased the average grain size and the grain size distribution.
- (2) Grain boundary energy and its misorientation dependence in the Fe-Sn alloy increased under a magnetic field. This is probably due to

suppression of Sn segregation to grain boundaries by a magnetic field.

- (3) Grain boundary energy in the 99.99% Fe increased with increasing temperature in a non-magnetic field. On the other hand the energy decreased with increasing temperature in a 6 T magnetic field. The opposite temperature coefficient observed could be explained by suppression of impurity segregation to grain boundaries by a magnetic field. In addition, the grain boundary energy discontinuously changed around the Curie temperature in a magnetic field.

#### ACKNOWLEDGEMENTS

The Authors would like to express their hearty thanks to Dr. T. Yamamuro (Kumamoto University) for useful advice for experiments, to Prof. M. Kawahara and Mr. Y. Hinokuma (Kumamoto University) for ICP analysis. This work was supported by a Grant-in-Aid for Basic Research (S) (19106013) and a Grant-in-Aid for JSPS Fellows (19-3284) from the Japan Society for the Promotion of Science (JSPS). These supports are greatly appreciated.

#### REFERENCES

- [1] G. Gottstein and L. S. Shvindlerman, *Grain Boundary Migration in Metals – Thermodynamics, Kinetics, Applications* (CRC Press, 1999).
- [2] S. Tsurekawa, T. Tanaka and H. Yoshinaga // *Mater. Sci. Eng. A* **176** (1994) 341.
- [3] C. G. Dunn and F. Lionetti // *Met. Trans.* (1949) 125.
- [4] W. T. Read and W. Shockley // *Phys. Rev.* **78** (1950) 275.
- [5] H. Gleiter and B. Chalmaers, *High-Angle Grain Boundaries* (Pergamon Press, 1972).
- [6] L. E. Murr, *Interfacial Phenomena in Metals and Alloys* (Addison-Wesley Pub.Comp, 1975).
- [7] A. Otsuki, H. Isono and M. Mizuno // *J. de Physique, Colloque C5*. **49** (1988) C5-563.
- [8] D. Wolf // *Phil. Mag. A*. **62** (1990) 447.
- [9] M. P. Seah and C. Lea // *Phil. Mag.* **31** (1975) 627.
- [10] H. Sautter, H. Gleiter and G. Baro // *Acta Metall.* **25** (1977) 467.
- [11] E. D. Hondros // *Proc. Roy. Soc.* **A286** (1965) 479.



- [12] R. Smoluchowski and R. W. Turner // *J. Appl. Phys.* **20** (1949) 745.
- [13] H. O. Martikainen and V. K. Lindroos // *Scandinavian J. Metall.* **10** (1981) 3.
- [14] T. Watanabe, Y. Suzuki, S. Tanii and H. Oikawa // *Phil. Mag. Lett.* **62** (1990) 9.
- [15] N. Masahashi, M. Matsuo and K. Watanabe // *J. Mater. Res.* **13** (1998) 457.
- [16] S. Bhaumik, X. Molodova, D. A. Molodov and G. Gottstein // *Scripta Mater.* **55** (2006) 995.
- [17] Y. Wu, X. Zhao, C-S. He, Y. D. Zhang, L. Zuo and C. Esling // *Mater. Trans.* **48** (2007), 2809.
- [18] T. Watanabe, In: *Proc. of the Fourth Intern. Conf. on Recrystallization and Related Phenomena* (The Japan Inst. Metals, 1999), p. 99.
- [19] K. Harada, S. Tsurekawa, T. Watanabe and G. Palumbo // *Scripta Mater.* **49** (2003) 367.
- [20] D. A. Molodov, C. Bollmann, P. Konijnenberg, L. A. Barrales-Mora and V. Mohles // *Mater. Trans.* **48** (2007), 2800.
- [21] H. Pender and R. L. Jones // *Phys. Rev.* **1** (1913) 259.
- [22] M. Shimotomai and K. Maruta // *Scripta Mater.* **42** (2000) 499.
- [23] J. – K. Choi, H. Ohtsuka, Y. Xu and W. – Y. Choo // *Scripta Mater.* **43** (2000) 221.
- [24] M. Shimotomai, K. Maruta, K. Mine and M. Matsui // *Acta Mater.* **51** (2003) 2921.
- [25] Y. D. Zhang, C. Esling, J. S. Lecomte, C. S. He, X. Zhao and L. Zuo // *Acta Mater.* **53** (2005) 5213.
- [26] S. Tsurekawa, K. Okamoto, K. Kawahara and T. Watanabe // *J. Mater. Sci.* **40** (2005) 895.
- [27] D. Gupta // *Interface Sci.* **11** (2003) 7.
- [28] P. Lejcek, S. Hofmann and V. Paidar // *Acta Mater.* **51** (2003) 3951.
- [29] P. Lejcek, S. Hofmann and J. Janovec // *Mater. Sci. Eng. A* **462** (2007) 76.